Energy Dissipation Analysis of Elastic-Plastic Materials

Han Yang[a], Sumeet Kumar Sinha[a], Yuan Feng[a], David B McCallen[b], Boris Jeremić[a,b,*]

[a] *Department of Civil and Environmental Engineering, University of California, Davis, CA, USA*
[b] *Earth Science Devision, Lawrence Berkeley National Laboratory, Berkeley, CA, USA*

Abstract

Presented is an energy dissipation analysis framework for granular material that is based on thermodynamics. Theoretical formulations are derived from the second law of thermodynamics, in conjunction with a few plausible assumptions on energy transformation and dissipation. The role of plastic free energy is emphasized by a conceptual experiment showing its physical nature. Theoretical formulation is adapted in order to be applied in elastic-plastic finite element method (FEM) simulations. Developed methodology is verified through comparison of input work, stored energy, and energy dissipation of the system. Separation of plastic work into plastic free energy and energy dissipation removes a common mistake, made in a number of publications, where energy dissipation can attain negative values (energy production) which is impossible.

Keywords: Seismic energy dissipation, FEM, Computational geomechanics, Thermodynamics, Elastic-plastic materials, Plastic free energy

---

[*] Corresponding author
Email address: `jeremic@ucdavis.edu` (Boris Jeremić)

Preprint submitted to Comput. Methods Appl. Mech. Engrg. *April 30, 2017*

1. Introduction

Energy dissipation in elastic plastic solids and structures is the result of an irreversible dissipative process in which energy is transformed from one form to another and entropy is produced. The transformation and dissipation of energy is related to permanent deformation and damage within an elastic-plastic material. Of particular interest here is the dissipation of mechanical energy that is input into elastic-plastic solids by static or dynamic excitations.

Early work on plastic dissipation was done by Farren and Taylor [16] and Taylor and Quinney [34]. They performed experiments on metals and proved that a large part, but not all, of the input mechanical energy is converted into heat. The remaining part of the non-recoverable plastic work is known as the stored energy of cold work. The ratio of plastic work converted into heating (Quinney–Taylor coefficient), usually denoted as β, has been used in most later work on this topic. Based on large number of experiments, this ratio was determined to be a constant between 0.6 to 1.0 [5, 2, 38, 13, 28, 26].

More recently Rittel [29, 30, 31] published several insightful papers on the energy dissipation (heat generation) of polymers during cyclic loading, presenting both experimental and theoretical works. Rosakis et al. [32] presented a constitutive model for metals based on thermoplasticity that is able to calculate the evolution of energy dissipation. Follow up papers [19, 27] present assumptions to simply the problem. One direct application of plastic dissipation to geotechnical engineering is presented by Veveakis et al. [36, 37], using thermoporomechanics to model the heating and pore pressure increase in large landslides, like the 1963 Vajont slide in Italy.

In the past few decades, extensive studies have been conducted on energy dissipation in structures and foundations. Work by Uang and Bertero [35] has been considered a source and a reference for many recent publications dealing with energy as a measure of structural demand. Uang and Bertero [35] developed an energy analysis methodology based on absolute input energy (or energy demand). Numerical analysis results were compared with experiments on a multi-story building. In their work, Uang and Bertero [35], calculated hysteretic energy indirectly by taking the difference of absorbed energy and elastic strain energy. The term absorbed energy of each time step is simply defined as restoring force times incremental displacement. It is also stated that hysteretic energy is irrecoverable, which indicates that this parameter was considered the same as hysteretic dissipation or plastic dissipation. An equation for energy balance, is given by (Uang and Bertero [35]) as:

$$E_i = E_k + E_\xi + E_a = E_k + E_\xi + E_s + E_h \tag{1}$$

where E_i is the (absolute) input energy, E_k is the (absolute) kinetic energy, E_ξ is the viscous damping energy, E_a is the absorbed energy, which is composed of elastic strain energy E_s and hysteretic energy E_h.

The problem with this approach is the absence of plastic free energy, which is necessary to correctly evaluate energy dissipation of elastic-plastic materials and to uphold the second law of thermodynamics. While there is no direct plot of plastic dissipation (hysteretic energy) in [35], since it was not defined directly, there are plots of other energy components. Plastic dissipation can be easily calculated from these plots. After doing this, indications of negative incremental energy dissipation, which violates the basic principles of thermodynamics, were found in various sections of the paper.

This misconception could be clarified by renaming hysteretic energy as plastic work, a sum of plastic dissipation and plastic free energy. Both plastic work and plastic free energy can be incrementally negative, but plastic dissipation (defined as the difference of plastic work and plastic free energy) must be incrementally non-negative during any time period. Unfortunately, this misconception has been inherited (if not magnified) by many following studies on energy analysis of earthquake soils and structures (hundreds of papers).

The basic principles of thermodynamics are frequently used to derive new constitutive models, for example by Dafalias and Popov [10], Ziegler and Wehrli [40], Collins and Houlsby [9], Houlsby and Puzrin [20], Collins [6], Collins and Kelly [8], Collins [7] and Feigenbaum and Dafalias [17]. The concept of plastic free energy is introduced to enforce the second law of thermodynamics for developed constitutive models. It is important to distinguish between energy dissipation due to plasticity and plastic work, which is often a source of a confusion. The physical nature of plastic free energy is illustrated later in this paper through a conceptual example that is analyzed on particle scale. Essentially, development of plastic free energy is caused by particle rearrangement in granular assembly under external loading.

Specific formulation of free energy depends on whether the elastic and plastic behavior of the material is coupled. According to Collins et al. [9], [6], [7], material coupling behavior can be divided into modulus coupling, where the instantaneous elastic stiffness (or compliance) moduli depend on the plastic strain, and dissipative coupling, where the rate of dissipation function depends not only on the plastic strains and their rates of change but also on the stresses (or equivalently the elastic strains). The modulus coupling describes the degradation of stiffness as in for rock and concrete, and is usually modeled by employing a coupled elastic-plastic constitutive model or by introducing damage variables. The dissipative coupling is considered to be one of the main reasons for non-associative behavior in geomaterials [9], [39].

A number of stability postulates are commonly used to prevent violation of principles of thermodynamics. Stability postulates include Drucker's stability condition [14], [15], Hill's stability condition [4], [18], and Il'Iushin's stability postulate [21], [24]. As summarized in a paper by Lade [23], theoretical considerations by Nemat–Nasser [25] and Runesson and Mrŏz [33] have suggested that they are sufficient but not necessary conditions for stability. These stability postulates can indeed ensure the admissibility of the constitutive models by assuming certain restrictions on incremental plastic work. As demonstrated by Collins [6], if the plastic strain rate is replaced by the irreversible stain rate in Drucker's postulate, then all the standard interpretations of the classical theory still apply for coupled materials. Dafalias [12] also modified Il'Iushin's postulate in a similar way and applied it to both coupled and uncoupled materials.

It is important to note that development of inelastic deformation in geomaterials involves large changes in entropy, and significant energy dissipation. It is thus useful to perform energy dissipation (balance) analysis for all models with inelastic deformation. In this paper we focus on energy dissipation on material level. Focus is on proper modeling that follows thermodynamics. Comparison is made between accumulated plastic dissipation and accumulated plastic work, since these quantities can be quite different in most cases. As a way of verification, the input work, which is introduced by applying external forces, is compared with the stored energy and dissipation in the entire system. Finally, conclusions on plastic energy dissipation are drawn from the verified results.

2. Theoretical and Computational Formulations

2.1. Thermo-Mechanical Theory

For energy analysis of elastic-plastic materials undergoing isothermal process, it is beneficial to start from the statement of the first and second laws of thermodynamics:

$$\hat{W} = \dot{\Psi} + \Phi \tag{2}$$

where $\Phi \geq 0$ and $\hat{W} \equiv \sigma : \dot{\epsilon} = \sigma_{ij}\dot{\epsilon}_{ij}$ is the rate of work per unit volume. The function Ψ is the Helmholtz free energy, and Φ is the rate of dissipation; both defined per volume. The free energy Ψ is a function of the state variables (also known as internal variables), but Φ and $\hat{W}$ are not the time derivatives of the state functions. The choice of state variables depends on the complexity of constitutive model that is being used, as cyclic loading with certain hardening behaviors usually requires more state variables. This will be elaborated in the following sections as we discuss specific elastic-plastic material models. Note that in this paper all stresses are defined as effective stresses. In order to avoid confusion, the common notation ($\sigma_{ij}^{'}$) will not be used. Standard definition of stress from mechanics of materials, i.e. positive in tension, is used.

For general elastic-plastic materials, the free energy depends on both the elastic and plastic strains. In most material models, it can be assumed that the free energy Ψ can be decomposed into elastic and plastic parts:

$$\Psi = \Psi_{el} + \Psi_{pl} \tag{3}$$

The total rate of work associated with the effective stress can be written as the sum of an elastic and plastic component:

$$\hat{W}^{el} \equiv \sigma_{ij}\dot{\epsilon}_{ij}^{el} = \dot{\Psi}_{el} \tag{4}$$

and

$$\hat{W}^{pl} \equiv \sigma_{ij}\dot{\epsilon}_{ij}^{pl} = \dot{\Psi}_{pl} + \Phi \tag{5}$$

In the case of a decoupled material, the elastic free energy Ψ_{el} depends only on the elastic strains, and the plastic free energy Ψ_{pl} depends only on the plastic strains, as shown by Collins and Houlsby [9]:

$$\Psi = \Psi_{el}(\epsilon_{ij}^{el}) + \Psi_{pl}(\epsilon_{ij}^{pl}) \tag{6}$$

The effective stress can also be decomposed into two parts:

$$\sigma_{ij} = \alpha_{ij} + \chi_{ij}, \quad \text{where } \alpha_{ij} \equiv \frac{\partial \Psi_{pl}}{\partial \epsilon_{ij}^{pl}} \quad \text{and} \quad \chi_{ij} \equiv \frac{\partial \Phi}{\partial \dot{\epsilon}_{ij}^{pl}} \tag{7}$$

The stress tensors α_{ij} and χ_{ij} are termed the shift (drag, back or quasi-conservative) stress and dissipative stress respectively.

Ziegler's orthogonal postulate [40] ensures the validity of Equation 7. It is equivalent to the maximum entropy production criterion, which is necessary to obtain unique formulation. Also, this is a weak assumption so that all the major continuum models of thermo-mechanics are included. Equation 5 of plastic work rate can hence be rewritten as:

$$\hat{W}^{pl} \equiv \sigma_{ij}\dot{\epsilon}_{ij}^{pl} = \dot{\Psi}_{pl} + \Phi = \alpha_{ij}\dot{\epsilon}_{ij}^{pl} + \chi_{ij}\dot{\epsilon}_{ij}^{pl} \tag{8}$$

The plastic work is the product of the true stress with the plastic strain rate, while the dissipation rate is the product of the dissipative stress with the plastic strain rate. They are only equal if the back stress is zero, or equivalently, if the free energy depends only on the elastic strains.

In kinematic hardening models, where the back stress describes the translation (or rotation) of the yield surface, the decomposition of the true stress (sum of back stress and dissipative stress) is a default assumption. Although such a shift stress is important for anisotropic material models, Collins and Kelly [8] have pointed out that it is also necessary in isotropic models of geomaterials with different strength in tension and compression.

2.2. Plastic Free Energy

A popular conceptual model, which focused on particulate materials and demonstrated the physical occurrence of shift stresses, was described by Besseling and Van Der Giessen [3] and Collins and Kelly [8]. On macro (continuum) scale, every point in a given element is at yield state and deforms plastically. But on meso-scale, only part of this element is undergoing plastic deformations, the remaining part is still within yield surface and respond elastically. The elastic strain energy stored in the elastic part of a plastically deformed macro-continuum element is considered to be locked into the macro-deformation, giving rise to the plastic free energy function Ψ_{pl} and its associated back stress α_{ij}. This energy can be released only when the plastic strains are reversed.

For better explanation, the nature of plastic free energy in particulate materials is illustrated through a finite element simulation combined with considerations of particle rearrangement on mesoscopic scale. Figure 1 shows stress-strain response of Drucker-Prager with nonlinear Armstrong-Frederick kinematic hardening, a typical elastic-plastic model for metals and geomaterials. Six states during shear are chosen to represent evolution of micro fabric of the numerical sample. Correspondingly, Figure 2 shows the process of particle rearrangement of the 2D granular assembly under cyclic shearing from microscopic level. The square window can be roughly considered as a representative volume (a constitutive level or a finite element) in FEM.

[Figure 1 about here.]

[Figure 2 about here.]

By discussing movement and energy of particle A in Figure 2, the physical nature of plastic free energy is illustrated. At state (a), which is the beginning of deformation, particle A does not bear any load other than its self weight. State (b) is in middle of loading, when particle B pushes downwards to particle A until it makes contact with particle D and E. Load reaches peak at state (c), and there's no space for particle A to move. Then the sample is unloaded to state (d). Particle A is now stuck between particles C, D, and F, which means that certain amount of elastic energy is stored due to particle elastic deformation. Compared with state (a), this part of elastic energy is not released when the sample is unloaded, which indicates that it's not classic strain energy. This part of elastic energy on particle level which can't be released by unloading is defined as the plastic free energy in granular materials. Reverse loading starts at state (e), where particle D pushes particle A upwards, making it squeeze through particle C and F. Elastic energy on particle level, which is now defined as plastic free energy, is released during reverse loading.

By analyzing this example, an explanation on particle scale is provided for the origin of plastic free energy in granular materials. It is important to note that the concept of plastic free energy also exists in metals and other materials, as studied by Dafalias et al. [11] and Feigenbaum and Dafalias [17]. The physical nature of plastic free energy in these materials can be different and probably should be studied on molecular and/or crystalline level.

Collins [8], [7] suggested that in the case of granular materials, the particle-level plastic energy dissipation during normal compaction, arises from the plastic deformations occurring at the inter-granular contacts on the strong force chains, that are bearing the bulk of the applied loads. Collins also suggested that the locked-in elastic energy is produced in the weak force networks, where the local stresses are not large enough to produce plastic deformation at the grain contacts. The plastic strains can be associated with the irreversible rearrangement of the particles, whilst the elastic energy arises from the elastic compression of the particle contacts. Part of this elastic strain energy will be released during unloading, however other part of this energy will be trapped as a result of the irreversible changes in the particle configuration.

2.3. Plastic Dissipation

As pointed out, plastic work and energy dissipation are not the same physical quantity. The confusion of these two concepts often leads to incorrect results and conclusions, especially in seismic energy dissipation analysis. Of major concern in this paper is the computation of plastic dissipation, as elaborated in this section.

With the decoupling assumption (Equation 6), the second law of thermodynamics (positive entropy production) directly leads to the dissipation inequality, which states that the energy dissipated due to the difference of the plastic work rate and the rate of the plastic part of the free energy must be non-negative:

$$\Phi = \sigma_{ij}\dot{\epsilon}_{ij}^{pl} - \dot{\Psi}_{pl} = \sigma_{ij}\dot{\epsilon}_{ij}^{pl} - \rho\dot{\psi}_{pl} \geq 0 \tag{9}$$

where $\dot{\psi}_{pl}$ is the rate of plastic free energy, per unit volume, and ρ is the density. In addition, ψ_{pl} denotes plastic free energy density, which is generally not constant at different locations in a body. This expression is closer to physics and makes it convenient for further derivations.

Now we proceed to consider how to calculate plastic free energy, which can then be used to calculate dissipation. According to Feigenbaum and Dafalias

[17], plastic free energy density ψ_{pl} is assumed to be additively decomposed into parts which correspond to the isotropic, kinematic and distortional hardening mechanisms as follows:

$$\psi_{pl} = \psi_{pl}^{iso} + \psi_{pl}^{ani}; \quad \psi_{pl}^{ani} = \psi_{pl}^{kin} - \psi_{pl}^{dis} \tag{10}$$

where ψ_{pl}^{iso}, ψ_{pl}^{ani}, ψ_{pl}^{kin}, and ψ_{pl}^{dis} are the isotropic, anisotropic, kinematic, and distortional parts of the plastic free energy, respectively. The anisotropic part is assumed to decompose into kinematic and distortional parts, which correspond to different hardening models. The subtraction, instead of addition, of ψ_{pl}^{dis} from ψ_{pl}^{kin}, to obtain the overall anisotropic part ψ_{pl}^{ani} of the plastic free energy, is a new concept proposed by Feigenbaum and Dafalias [17]. This expression can better fit experimental data, as well as satisfy the plausible expectations for a limitation of anisotropy development.

As pointed out by Dafalias et al. [11], the thermodynamic conjugates to each of the internal variables exist and each part of the plastic free energy can be assumed to be only a function of these conjugates. The explicit expressions for the isotropic and kinematic components of the plastic free energy are:

$$\psi_{pl}^{iso} = \psi_{pl}^{iso}(\bar{k}) = \frac{\kappa_1}{2\rho}\bar{k}^2; \quad \psi_{pl}^{kin} = \psi_{pl}^{kin}(\bar{\alpha}_{ij}) = \frac{a_1}{2\rho}\bar{\alpha}_{ij}\bar{\alpha}_{ij} \tag{11}$$

where $\bar{k}$ and $\bar{\alpha}_{ij}$ are the thermodynamic conjugates to k (size of the yield surface) and α_{ij} (deviatoric back stress tensor representing the center of the yield surface), respectively. Material constants κ_1 and a_1 are non-negative material constants whose values depend on the choice of elastic-plastic material models.

According to definition, the thermodynamic conjugates are related to the corresponding internal variables by:

$$k = \rho \frac{\partial \psi_{pl}^{iso}}{\partial \bar{k}} = \kappa_1 \bar{k}; \quad \alpha_{ij} = \rho \frac{\partial \psi_{pl}^{kin}}{\partial \bar{\alpha}_{ij}} = a_1 \bar{\alpha}_{ij} \tag{12}$$

By substituting Equation 12 back into Equation 11, the plastic free energy can be expressed in terms of the internal variables:

$$\psi_{pl}^{iso} = \frac{1}{2\rho\kappa_1} k^2; \quad \psi_{pl}^{kin} = \frac{1}{2\rho a_1} \alpha_{ij}\alpha_{ij} \tag{13}$$

With Equation 13, the components of plastic free energy can be computed, as long as the internal variables are provided. Combining Equation 9 with 13, the plastic dissipation in a given elastic-plastic material can be accurately obtained at any location, at any time. This approach allows engineers and designers to correctly identify energy dissipation in time and space and make appropriate conclusions on material behavior.

2.4. Energy Computation in Finite Elements

Formulations from the previous section are applied to FEM analysis in order to follow energy dissipation. Energy density is chosen as the physical parameter for energy analysis. Energy density in this study is defined as the amount of energy stored in a given region of space per unit volume.

For FEM simulations, both external forces and displacements can be prescribed. The finite element program accepts either (or both) forces and/or displacements as input and solves for the other. Either way, the rate of input work can be calculated by simply multiplying force and displacement within a time step. Therefor input work of a finite element model is:

$$W_{Input}(t) = \int_0^t \dot{W}_{Input}(T) dT = \int_0^t \sum_i F_i^{ex}(\boldsymbol{x}, T) \dot{u}_i(\boldsymbol{x}, T) dT \tag{14}$$

where F_i^{ex} is the external force and u_i is the displacement computed at the location of the applied load, at given time step, for a load controlled analysis.

The external load can have many forms, including nodal loads, surface loads, and body loads. All of them are ultimately transformed into nodal forces. As shown in Equation 14, input work is computed incrementally at each time step, in order to obtain the evolution of total input work at certain time.

As shown in Figure 3, when loads and/or displacements are introduced into a finite element model, the input energy will be converted in a number of different forms as it propagates through the system. Input energy will be converted into kinetic energy, free energy, and dissipation. As mentioned before, free energy can be further separated into elastic part, which is traditionally defined as strain energy, and plastic part, which is defined as the plastic free energy. Kinetic energy and strain energy can be considered as the recoverable portion of the total energy since they are transforming from one to another. Plastic free energy is more complicated in the sense that it is conditionally recoverable during reverse loading, as has been discussed in detail in previous sections. Other than kinetic energy and free energy, the rest of the input energy is dissipated, transformed into heat or other forms of energy that are irrecoverable.

[Figure 3 about here.]

Calculation of kinetic energy and strain energy is rather straight forward:

$$U_K(\boldsymbol{x}, t) = \frac{1}{2}\rho \dot{u}_{ij}(\boldsymbol{x}, t)\dot{u}_{ij}(\boldsymbol{x}, t) \tag{15}$$

$$U_S(\boldsymbol{x}, t) = \int_0^t \dot{U}_S(\boldsymbol{x}, T)dT = \int_0^t \sigma_{ij}(\boldsymbol{x}, T)\dot{\epsilon}_{ij}^{el}(\boldsymbol{x}, T)dT \tag{16}$$

where U_K and U_S are the kinetic energy density and strain energy density, respectively.

Similar to the input energy, strain energy density and plastic free energy are also computed incrementally. Integrating energy density over the entire model, corresponding energy quantities are expressed as:

$$E_K(t) = \int_V U_K(\boldsymbol{x}, t) dV \tag{17}$$

$$E_S(t) = \int_V U_S(\boldsymbol{x}, t) dV \tag{18}$$

$$E_P(t) = \int_V \Psi_{pl}(\boldsymbol{x}, t) dV \tag{19}$$

where E_K, E_S, and E_P are the kinetic energy, strain energy, and plastic free energy of the entire model, respectively. Energy densities, defined in Equations 15 and 16 are functions of both time and space, while energy components, defined in the above equations (Equation 17, 18, and 19) are only functions of time, since they are integrated over the whole model.

Although the plastic free energy is conditionally recoverable, it is still considered to be stored in the system, rather than dissipated. Summing up all the stored energy E_{Stored}, one obtains:

$$E_{Stored} = E_K + E_S + E_P \tag{20}$$

Rate of plastic dissipation, given by Equation 9, can be integrated over time and space:

$$D_P(t) = \int_V \int_0^t \Phi(\boldsymbol{x}, T) dT dV \tag{21}$$

where D_P is the dissipation due to plasticity of the entire model at certain time.

Finally the energy balance of a finite element model is given by:

$$W_{Input} = E_{Stored} + D_P = E_K + E_S + E_P + D_P \tag{22}$$

3. Numerical Studies

Numerical simulation results presented in this paper are performed using the Real ESSI (Real Earthquake Soil Structure Interaction) Simulator [22]. Examples in this paper focus on constitutive behavior of elastic-plastic material from the perspective of energy dissipation. All cases are modeled with solid brick elements, using static, load control analysis.

3.1. Elastic Material

[Figure 4 about here.]

Initial investigation of energy dissipation is focused on linear elastic material. It is noted that linear elastic material does not dissipate energy. However, use of linear elastic material model is suitable for preliminary verification of the newly developed energy analysis methodology. In this section, energy balance in a single brick element and a cantilever beam is studied, as shown in Figure 4.

The simplest case is a single element model under uniform shear load. The model is constrained appropriately to simulate simple shear test. In order to show the influence of different material parameters and loads, a set of simulations are performed and the results are presented in Table 1 and Figure 5.

[Table 1 about here.]

[Figure 5 about here.]

Since linear elastic material is used with static algorithm, energy components related to dynamics (kinetic energy) and plasticity (plastic free energy and plastic dissipation) are equal to zero. This means that all input work is stored in the system, as observed in all cases.

Figure 5 shows that energy stored in the system is inversely proportional to Young's moduli and proportional to Poisson's ratio. This is expected because of the following equations for strain energy under static shear loading:

$$E_S = \frac{1}{2}\tau\gamma = \frac{1}{2G}\tau^2 = \frac{1+\nu}{E}\tau^2 \tag{23}$$

Note that these relationships are only valid at constitutive level. For models with more finite elements, stress and strain are generally not uniform. The computation of energy depends on the distribution of energy density, and nonuniform stress/strain distribution will result in nonuniform energy density distribution.

In order to study the influence of simulation parameters in larger models, another set of simulations with cantilever model (Figure 4b) are performed. Vertical loads are applied to the nodes of the free end. In this case, both shearing and bending occurs, which means that in general a full 3D state of stress and strain is present. The results are presented in Table 2 and Figure 5. As expected, energy behavior of cantilever is different than the single-element/constitutive example.

[Table 2 about here.]

For all cases, the energy balance between input and storage is maintained, which gives us confidence on the energy calculation methodology for elastic material. According to results in Figure 5, energy stored in the system is still inversely proportional to Young's modulus. This is because the general equation for elastic strain energy density is:

$$E_S = \frac{1}{2E}\left(\sigma_{xx}^2 + \sigma_{yy}^2 + \sigma_{zz}^2 + 2(1+\nu)(\sigma_{xy}^2 + \sigma_{yz}^2 + \sigma_{zx}^2)\right) \tag{24}$$

So as long as all the elements have the same Young's modulus, the relationship between stored energy and Young's modulus will remain valid.

3.2. Elastic-Perfectly Plastic Material

In this section, elastic-perfectly plastic material is used. Equations 9 and 13 indicate that in the case of no hardening the rate of plastic free energy is zero. Then the incremental plastic work is equal to incremental plastic dissipation. Note that this is one of the rare cases where plastic dissipation equals to plastic work.

Figure 6 shows stress–strain curve (left) and energy calculated for elastic-perfectly plastic constitutive model (right) used here.

[Figure 6 about here.]

In this case, the plastic dissipation is equal to the plastic work. This means that the plastic free energy does not develop at all during loading and unloading. Zero plastic free energy points out the absence of fabric evolution of a particulate, elastic-plastic material, as all the input work is dissipated through particle to particle friction. Since there is no plastic free energy E_P in this case, the stored energy equals to mechanical energy, which is the combination of strain energy E_S and kinetic energy E_K. Total stored energy E_{Stored} develops nonlinearly and always has the same value at the beginning of every loop after the first one. Plastic dissipation D_P increases linearly when the material yields. This can be explained by rewriting Equation 9 with $\Psi_{pl} = 0$:

$$\Phi = \sigma_{ij} \dot{\epsilon}_{ij}^{pl} \tag{25}$$

where stress σ_{ij} is constant after elastic perfectly plastic material yields, and rate plastic deformation $\dot{\epsilon}_{ij}^{pl}$ is also constant. Then the rate of plastic dissipation is constant which makes the plastic dissipation D_P increase linearly.

3.3. Elastic-Plastic Material with Isotropic Hardening

Next material model used is elastic-plastic with linear isotropic hardening. First used to model monotonic behavior of elastic-plastic materials, isotropic hardening assumes that the yield surface maintains shape, while isotropically (proportionally) changing its size. Figure 7 illustrates the stress-strain response as well as energy balance for elastic-plastic material with isotropic hardening.

[Figure 7 about here.]

As can be observed from Figure 7, plastic free energy is equal to the plastic work, which means that the plastic dissipation is zero during cycles of loading. Even though this might sound surprising, it can be explained using basic thermodynamics. Linear isotropic hardening, used in this case, can be described through a rate of the internal variable (size of the yield surface) $\dot{k}$ as:

$$\dot{k} = \kappa_1 |\dot{\epsilon}_{ij}^{pl}| \tag{26}$$

where $|\dot{\epsilon}_{ij}^{pl}|$ is the magnitude of the rate of plastic strain while κ_1 is a hardening constant. Substituting previous equation into Equation 13 yields:

$$\psi_{pl} = \psi_{pl}^{iso} = \frac{\kappa_1}{2\rho} \epsilon_{ij}^{pl} \epsilon_{ij}^{pl} \tag{27}$$

Take the time derivative of the above equation:

$$\dot{\psi}_{pl} = \frac{\kappa_1}{\rho} \epsilon_{ij}^{pl} \dot{\epsilon}_{ij}^{pl} \tag{28}$$

Then the rate of dissipation due to plasticity can be expressed as:

$$\Phi = \sigma_{ij}\epsilon_{ij}^{pl} - \rho\dot{\psi}_{pl} = (\sigma_{ij} - \kappa_1\epsilon_{ij}^{pl})\dot{\epsilon}_{ij}^{pl} = (\sigma_{ij} - km_{ij})\dot{\epsilon}_{ij}^{pl} \tag{29}$$

where m_{ij} is the plastic flow direction. The plastic flow direction defines the direction of incremental plastic strain, which can be different from the direction of total plastic strain. But in the case of von Mises type elastic-plastic material with only isotropic hardening, whose yield surface is always a circle with center at the origin, the plastic flow direction m_{ij} is the same as the direction of the total plastic strain ϵ_{ij}^{pl}. Thus we have $\kappa_1\epsilon_{ij}^{pl} = km_{ij}$ in the above equation.

If we assume, for simplicity sake, that plastic flow direction is associated with the yield function, that is there is only deviatoric plastic flow, as yield function is of von Mises type, the gradient of the yield surface $n_{ij}(= \partial F/\partial\sigma_{ij})$ is equal to the plastic flow direction $m_{ij}(= n_{ij})$. Noting that $\sigma_{ij}\dot{\epsilon}_{ij}^{pl} = s_{ij}\dot{\epsilon}_{ij}^{pl}$, where $s_{ij}(= \sigma_{ij} - 1/3\sigma_{kk})$ is the deviatoric part of the stress tensor, the rate of plastic dissipation can be rewritten as:

$$\Phi = (s_{ij} - kn_{ij})\dot{\epsilon}_{ij}^{pl} = \alpha_{ij}\dot{\epsilon}_{ij}^{pl} \tag{30}$$

Realizing that the back stress α_{ij} is always zero since we assume no kinematic hardening, then the rate of plastic dissipation becomes zero, which means there is no energy dissipation during cycles of loading for isotropically hardening material. Obviously, the observed response is not physical from the perspective of energy dissipation. Therefore, isotropic hardening material models cannot properly model energy dissipation, even for monotonic loading.

3.4. Elastic-Plastic Material with Kinematic Hardening

Compared with isotropic hardening, kinematic hardening can better describe the constitutive, stress-strain behavior of elastic-plastic materials, particularly for cyclic loading. Elastic-plastic material that relies on kinematic hardening is used to analyze energy dissipation. Both linear and nonlinear kinematic hardening rules are investigated in relation to energy dissipation.

3.4.1. Prager Linear Kinematic Hardening

Prager's linear kinematic hardening rule is given as:

$$\dot{\alpha}_{ij} = a_1 \dot{\epsilon}^{pl}_{ij} \tag{31}$$

where a_1 is a hardening constant. If only linear kinematic hardening (Equation 31) is assumed, the back stress α_{ij} is expressed explicitly, and can be substituted into Equation 13 yielding:

$$\psi_{pl} = \psi^{kin}_{pl} = \frac{a_1}{2\rho} \epsilon^{pl}_{ij} \epsilon^{pl}_{ij} \tag{32}$$

Take the time derivative of the above equation:

$$\dot{\psi}_{pl} = \frac{a_1}{\rho} \epsilon^{pl}_{ij} \dot{\epsilon}^{pl}_{ij} \tag{33}$$

If we again assume that the gradient of the yield surface n_{ij} is equal to the plastic flow direction m_{ij}, as in the case of linear isotropic hardening, then the rate of dissipation due to plasticity can be rewritten as:

$$\Phi = \sigma_{ij} \dot{\epsilon}^{pl}_{ij} - \rho \dot{\psi}_{pl} = (s_{ij} - \alpha_{ij}) \dot{\epsilon}^{pl}_{ij} = k m_{ij} \dot{\epsilon}^{pl}_{ij} \tag{34}$$

Notice that the term $m_{ij} \dot{\epsilon}^{pl}_{ij}$ denotes the magnitude of the rate of plastic strain. Since only linear kinematic hardening is assumed, the internal variable k will remain constant. So if loads are applied in such a way that the rate of plastic strain is constant, then the rate of dissipation will also remain constant. In other words, the accumulated dissipation will be linearly increasing under the assumption of linear kinematic hardening.

Figure 8 shows stress–strain response (left) and energy computation results (right) of an elastic-plastic material with linear kinematic hardening.

[Figure 8 about here.]

As expected, the plastic dissipation increases linearly once the material yields. In contrast to the isotropic hardening case, a significant amount of the input work is dissipated due to material plasticity. The ratio of dissipated energy to input work is largely influenced by the material parameters. However, in general, energy dissipation will be observed if kinematic hardening model is used.

Another important observation is that the plastic work decreases during certain phases of reverse loading, while the actual rate of energy dissipation is always nonnegative. It is important not to confuses the definitions of plastic work to plastic dissipation, as plastic work can increase and decrease which can lead to a (impossible) conclusion, violating the second law of thermodynamics.

3.4.2. Armstrong-Frederick Kinematic Hardening

Armstrong-Frederick kinematic hardening model [1] is often used to simulate elastic-plastic material behavior under cyclic loading. Material parameters of the Armstrong Frederic kinematic hardening rule can be derived from basic thermodynamics.

Feigenbaum and Dafalias [17] gave the sufficient (but not necessary) conditions of the inequality in Equation 9. These conditions are more restrictive but satisfy the frameworks of most classical elastic-plastic models. One of the sufficient conditions corresponds to kinematic hardening is expressed as:

$$\alpha_{ij}(\dot{\epsilon}_{ij}^{pl} - \frac{1}{a_1}\dot{\alpha}_{ij}) \geq 0 \tag{35}$$

The following relation is a sufficient condition to satisfy Equation 35:

$$\dot{\alpha}_{ij} = a_1\dot{\epsilon}_{ij}^{pl} - a_2\dot{\lambda}\alpha_{ij} \tag{36}$$

where $\dot{\lambda}$ is a non-negative scalar plastic multiplier and a_2 is a non-negative material hardening constant. It can be proven that a_1/a_2 is related to the limit of back stress magnitude $|\alpha_{ij}|$. Equation 36 should be recognized as the classical Armstrong-Frederick nonlinear kinematic hardening.

Taking the time derivative of the kinematic part of plastic free energy (Equation 33), and substituting the expression of back stress α_{ij} (Equation 36) gives:

$$\dot{\psi}_{pl}^{kin} = \frac{1}{\rho a_1}\alpha_{ij}\dot{\alpha}_{ij} = \frac{1}{\rho}\alpha_{ij}(\dot{\epsilon}_{ij}^{pl} - \frac{a_2}{a_1}\dot{\lambda}\alpha_{ij}) \tag{37}$$

If the gradient of the yield surface n_{ij} is assumed to be equal to the plastic flow direction m_{ij}, as was done in previous sections, then the rate of plastic energy dissipation of an Armstrong-Frederick kinematic hardening elastic-plastic material is given by:

$$\Phi = \sigma_{ij}\dot{\epsilon}_{ij}^{pl} - \rho\dot{\psi}_{pl} = s_{ij}\dot{\epsilon}_{ij}^{pl} - \alpha_{ij}\dot{\epsilon}_{ij}^{pl} + \frac{a_2}{a_1}\dot{\lambda}\alpha_{ij}\alpha_{ij} = km_{ij}\dot{\epsilon}_{ij}^{pl} + \frac{a_2}{a_1}\dot{\lambda}\alpha_{ij}\alpha_{ij} \tag{38}$$

Compared with Equation 34, the above expression has an additional term which makes the rate of plastic dissipation non-constant even if the rate of plastic strain is constant. As the back stress α_{ij} becomes larger when load increases, the rate of plastic dissipation also increases. This indicates a nonlinear result of total plastic dissipation, which is exactly what we have observed in our computations.

[Figure 9 about here.]

Figure 9 shows the energy computation results of an elastic-plastic material with Armstrong-Frederick kinematic hardening. Compared to all previous cases, the material response of this model is more sophisticated and more realistic. Decrease of plastic work is observed, again, while the plastic dissipation is always nonnegative during the entire simulation. For both linear and nonlinear kinematic hardening cases, the plastic free energy is relatively small compared to the plastic dissipation.

4. Conclusions

Presented was a methodology for (correct) computation of energy dissipation in elastic-plastic materials based on the second law of thermodynamics. A very important role of plastic free energy was analyzed, with highlights on its physical nature and theoretical formulations. The proposed methodology has been illustrated using a number of elasto-plastic material models.

An analysis of a common misconception that equates plastic work and dissipation, which leads to the violation of the basic principles of thermodynamics, was addressed. A conceptual example, for granular materials, was used to explain the physical meaning of plastic free energy. It was also shown that plastic free energy is responsible for the evolution of internal variables.

It was shown that energy balance is ensured by taking into consideration all energy components, including kinetic and strain energy. Input work was balanced with the stored and dissipated energy, expressed as the summation of all possible components.

Presented approach was illustrated and tested using several elastic-plastic constitutive models with various hardening rules. Elastic materials showed no energy dissipation (as expected), leading to the input work being equal to the stored energy. Elastic-perfectly plastic materials had no change in plastic free energy, which led to the equality of plastic work and plastic dissipation and indicated no evolution of particle arrangements. The plastic dissipation, in that case, was observed to be increasing linearly. Isotropic hardening materials experienced zero dissipation even after yielding. This observation was surprising, but verified by further derivation of energy equations. This observation also serves as a reminder that the isotropic hardening rules can be used, but only with observed lack of energy dissipation. Prager's linear and Armstrong-Frederick nonlinear kinematic hardening materials both gave significant dissipations, with large fluctuation of plastic free energy as well. In the case with linear kinematic hardening, linear increase of dissipation was derived and observed, while energy was dissipated nonlinearly in the case of nonlinear kinematic hardening. Although the plastic free energy was not significant for some materials, it is noted that it should always be recognized and considered during energy analysis, so that the basic principles of thermodynamics are maintained.

5. Acknowledgments

This work was supported by the US-DOE. We would like to thank Professor Yannis Dafalias (UCD and NTUA) for inspiring discussions.

References

[1] P. Armstrong and C. Frederick. A mathematical representation of the multiaxial bauschinger effect. Technical Report RD/B/N/ 731,, C.E.G.B., 1966.

[2] T. Belytschko, B. Moran, and M. Kulkarni. On the crucial role of imperfections in quasi-static viscoplastic solutions. *Journal of Applied Mechanics*, 58:658–665, 1991.

[3] J. F. Besseling and E. Van Der Giessen. *Mathematical modeling of inelastic deformation*, volume 5. CRC Press, 1994.

[4] J. Bishop and R. Hill. A theory of the plastic distortion of a polycrystalline aggregate under combined stresses. *The London, Edinburgh, and Dublin Philosophical Magazine and Journal of Science*, 42(327):414–427, 1951.

[5] R. Clifton, J. Duffy, K. Hartley, and T. Shawki. On critical conditions for shear band formation at high strain rates. *Scripta Metallurgica*, 18 (5):443–448, 1984.

[6] I. Collins. Associated and non-associated aspects of the constitutive laws for coupled elastic/plastic materials. *International Journal of Geomechanics*, 2(2):259–267, 2002.

[7] I. Collins. A systematic procedure for constructing critical state models in three dimensions. *International Journal of Solids and Structures*, 40 (17):4379–4397, 2003.

[8] I. Collins and P. Kelly. A thermomechanical analysis of a family of soil models. *Geotechnique*, 52(7):507–518, 2002.

[9] I. F. Collins and G. T. Houlsby. Application of thermomechanical principles to the modelling of geotechnical materials. *Procedings of Royal Society London*, 453:1975–2001, 1997.

[10] Y. Dafalias and E. Popov. A model of nonlinearly hardening materials for complex loading. *Acta mechanica*, 21(3):173–192, 1975.

[11] Y. Dafalias, D. Schick, C. Tsakmakis, K. Hutter, and H. Baaser. A simple model for describing yield surface evolution. In *Lecture note in applied and computational mechanics*, pages 169–201. Springer, 2002.

[12] Y. F. Dafalias. Il'iushin's postulate and resulting thermodynamic conditions on elastic–plastic coupling. *International Journal of Solids and Structures*, 13:239–251, 1977.

[13] M. Dolinski, D. Rittel, and A. Dorogoy. Modeling adiabatic shear failure from energy considerations. *Journal of the Mechanics and Physics of Solids*, 58(11):1759–1775, 2010.

[14] D. C. Drucker. On uniqueness in the theory of plasticity. *Quarterly of Applied Mathematics*, pages 35–42, 1956.

[15] D. C. Drucker. A definition of stable inelastic material. Technical report, DTIC Document, 1957.

[16] W. Farren and G. Taylor. The heat developed during plastic extension of metals. In *Proceedings of the royal society of London A: mathematical, physical and engineering sciences*, volume 107, pages 422–451. The Royal Society, 1925.

[17] H. P. Feigenbaum and Y. F. Dafalias. Directional distortional hardening in metal plasticity within thermodynamics. *International Journal of Solids and Structures*, 44(22-23):7526–7542, 2007.

[18] R. Hill. A general theory of uniqueness and stability in elastic-plastic solids. *Journal of the Mechanics and Physics of Solids*, 6(3):236–249, 1958.

[19] J. Hodowany, G. Ravichandran, A. Rosakis, and P. Rosakis. Partition of plastic work into heat and stored energy in metals. *Experimental mechanics*, 40(2):113–123, 2000.

[20] G. Houlsby and A. Puzrin. A thermomechanical framework for constitutive models for rate-independent dissipative materials. *International Journal of Plasticity*, 16(9):1017–1047, 2000.

[21] A. Il'Iushin. On the postulate of plasticity. *Journal of Applied Mathematics and Mechanics*, 25(3):746–752, 1961.

[22] B. Jeremić, G. Jie, Z. Cheng, N. Tafazzoli, P. Tasiopoulou, F. P. J. A. Abell, K. Watanabe, Y. Feng, S. K. Sinha, F. Behbehani, and H. Yang. *The Real ESSI Simulator System*. University of California, Davis and Lawrence Berkeley National Laboratory, 2016. `http://sokocalo.engr.ucdavis.edu/~jeremic/Real_ESSI_Simulator/`.

[23] P. V. Lade. Instability, shear banding, and failure in granular materials. *International Journal of Solids and Structures*, 39(13):3337–3357, 2002.

[24] J. Lubliner. *Plasticity Theory*. Macmillan Publishing Company, New York., 1990.

[25] S. Nemat–Nasser. On finite plastic flow of crystalline solids and geomaterials. *Journal of Applied Mechanics*, 50:1114–1126, 1983.

[26] S. Osovski, D. Rittel, and A. Venkert. The respective influence of microstructural and thermal softening on adiabatic shear localization. *Mechanics of Materials*, 56:11–22, 2013.

[27] G. Ravichandran, A. J. Rosakis, J. Hodowany, P. Rosakis, M. D. Furnish, N. N. Thadhani, and Y. Horie. On the conversion of plastic work into heat during high-strain-rate deformation. In *AIP conference proceedings*, volume 620, pages 557–562. AIP, 2002.

[28] B. Ren and S. Li. Meshfree simulations of plugging failures in high-speed impacts. *Computers & structures*, 88(15):909–923, 2010.

[29] D. Rittel. An investigation of the heat generated during cyclic loading of two glassy polymers. part i: Experimental. *Mechanics of Materials*, 32(3):131–147, 2000.

[30] D. Rittel and Y. Rabin. An investigation of the heat generated during cyclic loading of two glassy polymers. part ii: Thermal analysis. *Mechanics of Materials*, 32(3):149–159, 2000.

[31] D. Rittel, N. Eliash, and J. Halary. Hysteretic heating of modified poly (methylmethacrylate). *Polymer*, 44(9):2817–2822, 2003.

[32] P. Rosakis, A. Rosakis, G. Ravichandran, and J. Hodowany. A thermodynamic internal variable model for the partition of plastic work into heat and stored energy in metals. *Journal of the Mechanics and Physics of Solids*, 48(3):581–607, 2000.

[33] K. Runesson and Z. Mrŏz. A note on nonassociated plastic flow rules. *International Journal of Plasticity*, 5:639–658, 1989.

[34] G. I. Taylor and H. Quinney. The latent energy remaining in a metal after cold working. *Proceedings of the Royal Society of London. Series A, Containing Papers of a Mathematical and Physical Character*, 143 (849):307–326, 1934.

[35] C.-M. Uang and V. V. Bertero. Evaluation of seismic energy in structures. *Earthquake Engineering & Structural Dynamics*, 19(1):77–90, 1990.

[36] E. Veveakis, I. Vardoulakis, and G. Di Toro. Thermoporomechanics of creeping landslides: The 1963 vaiont slide, northern italy. *Journal of Geophysical Research: Earth Surface*, 112(F3), 2007.

[37] E. Veveakis, J. Sulem, and I. Stefanou. Modeling of fault gouges with cosserat continuum mechanics: Influence of thermal pressurization and chemical decomposition as coseismic weakening mechanisms. *Journal of Structural Geology*, 38:254–264, 2012.

[38] M. Zhou, G. Ravichandran, and A. Rosakis. Dynamically propagating shear bands in impact-loaded prenotched platesii. numerical simulations. *Journal of the Mechanics and Physics of Solids*, 44(6):1007–1032, 1996.

[39] H. Ziegler. Discussion of some objections to thermomechanical orthogonality. *Ingenieur-Archiv*, 50(3):149–164, 1981.

[40] H. Ziegler and C. Wehrli. The derivation of constitutive relations from the free energy and the dissipation function. *Advances in applied mechanics*, 25:183–238, 1987.

List of Figures

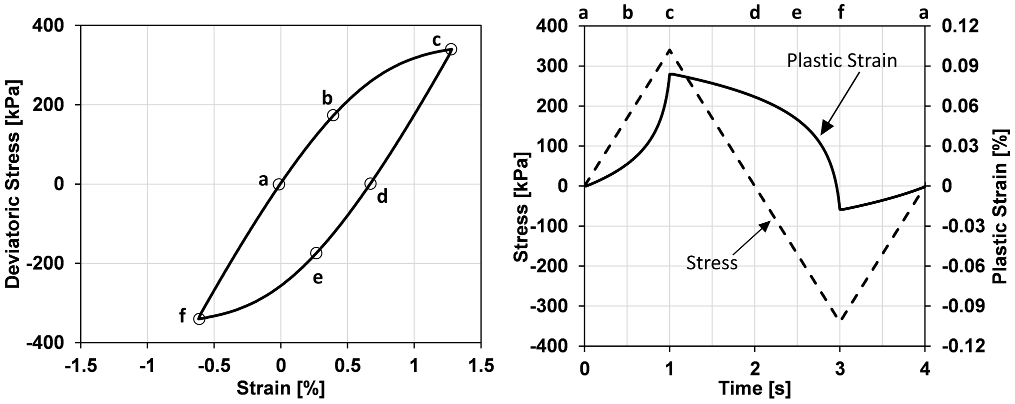

(a) (b)

Figure 1: Elastic-plastic material modeled with Drucker-Prager yield function and Armstrong-Frederick kinematic hardening under cyclic shear loading: (a) Stress-strain curve; (b) stress and plastic strain versus time.

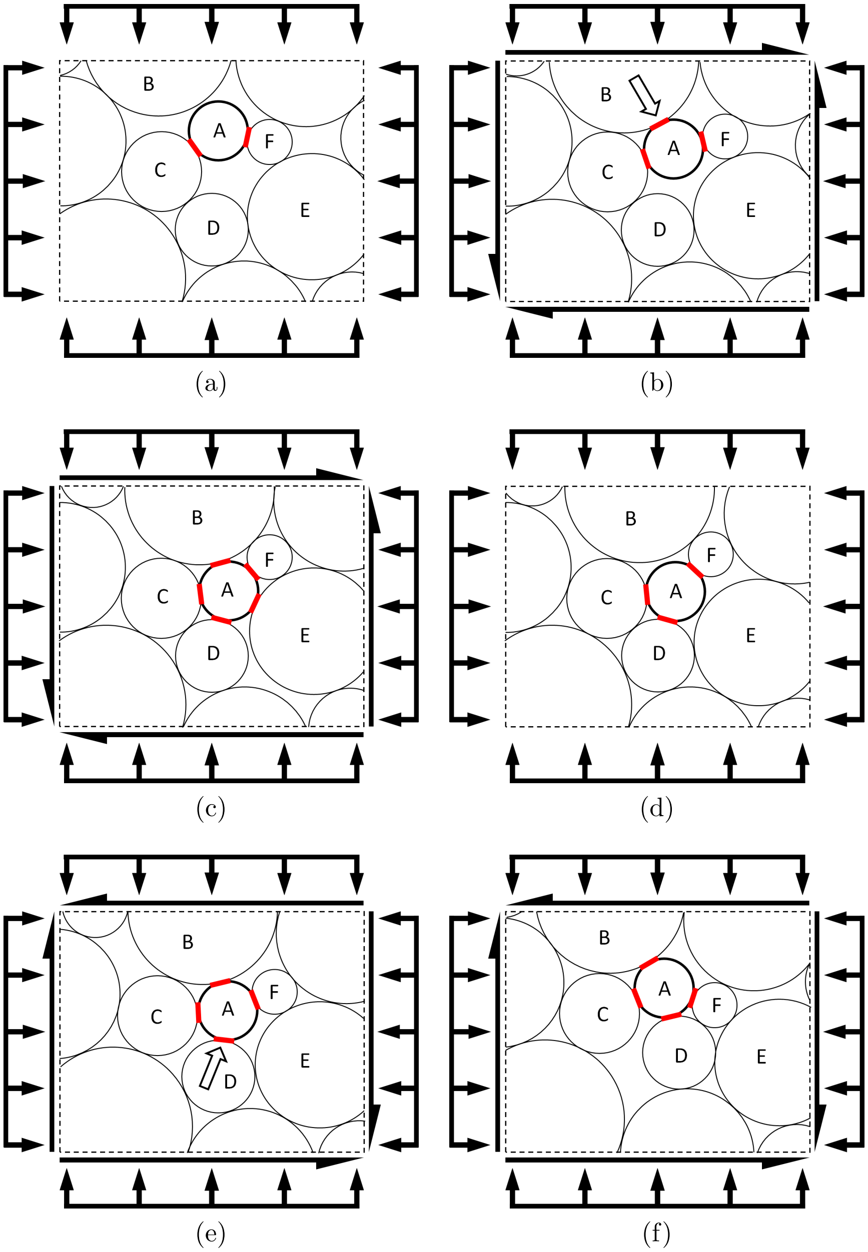

Figure 2: Particle rearrangement of a 2D granular assembly under cyclic shearing: (a) Initial state; (b) Loading (accumulating plastic free energy); (c) End of loading (maximum plastic free energy); (d) Unloading (plastic free energy unchanged); (e) Reverse loading (releasing plastic free energy); (f) End of reverse loading (plastic free energy released).

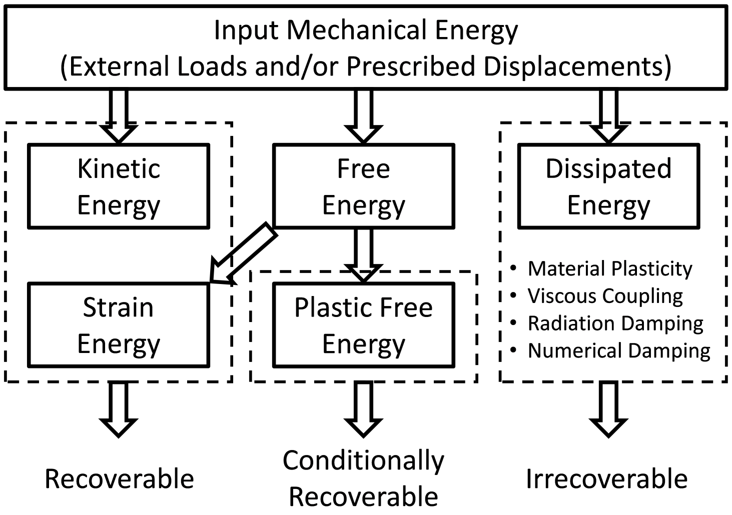

Figure 3: Different forms of energy in a dynamic soil-structure system.

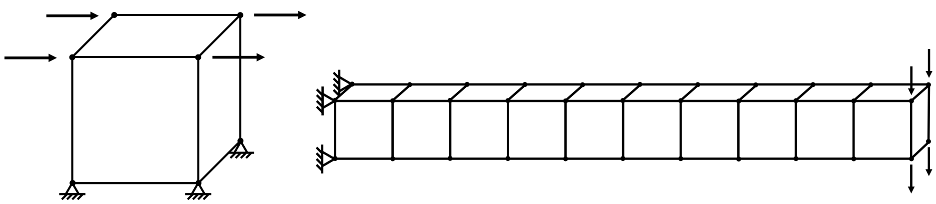

(a) (b)

Figure 4: Numerical models used in this paper: (a) Single brick element; (b) Cantilever with 10 brick elements.

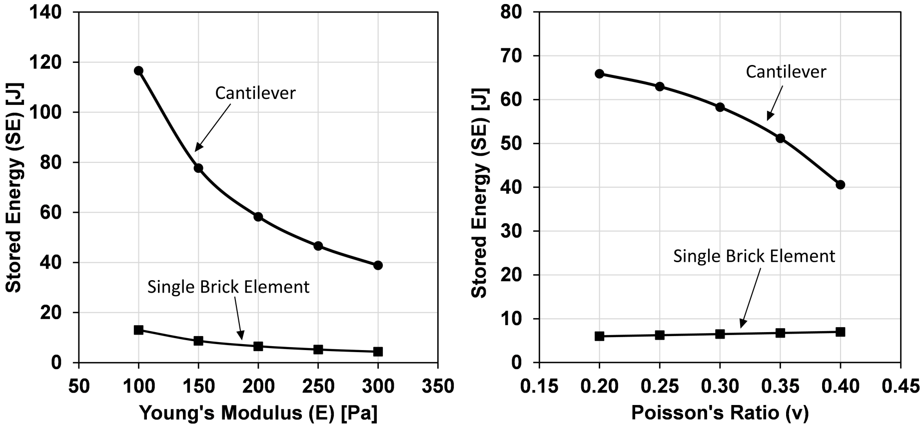

(a) (b)

Figure 5: Relationships between energy storage and different simulation parameters (single element model): (a) Young's modulus; (b) Poisson's ratio.

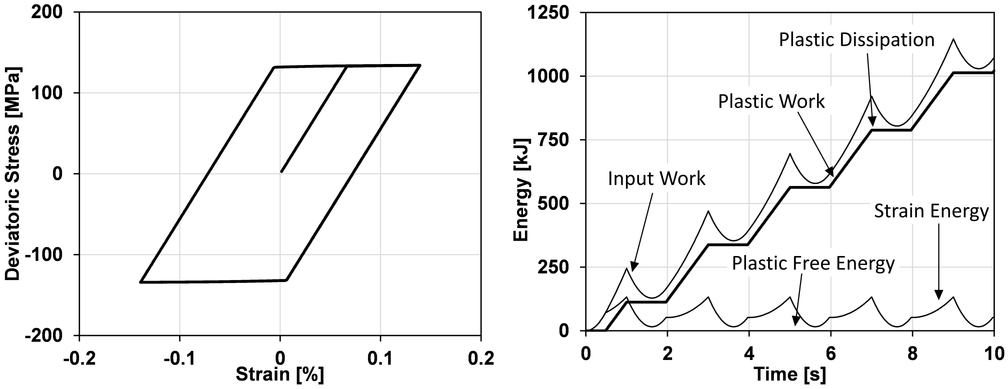

(a) (b)

Figure 6: Energy analysis of elastic perfectly plastic material: (a) Stress–strain curve; (b) Input work, plastic dissipation, strain energy and plastic work.

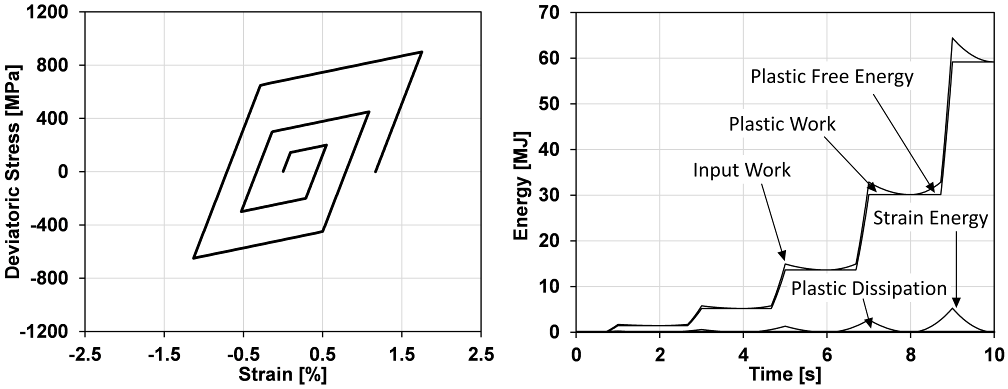

(a) (b)

Figure 7: Energy analysis of elastic-plastic material with isotropic hardening: (a) Stress-strain curve; (b) Input work, plastic dissipation, strain energy, and plastic work.

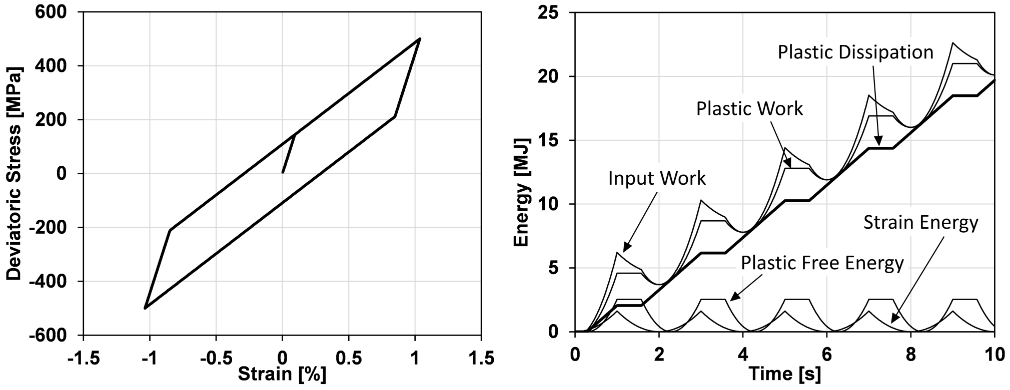

(a) (b)

Figure 8: Energy analysis of elastic-plastic material with linear kinematic hardening: (a) Stress–strain curve; (b) Input work, plastic dissipation strain energy and plastic work.

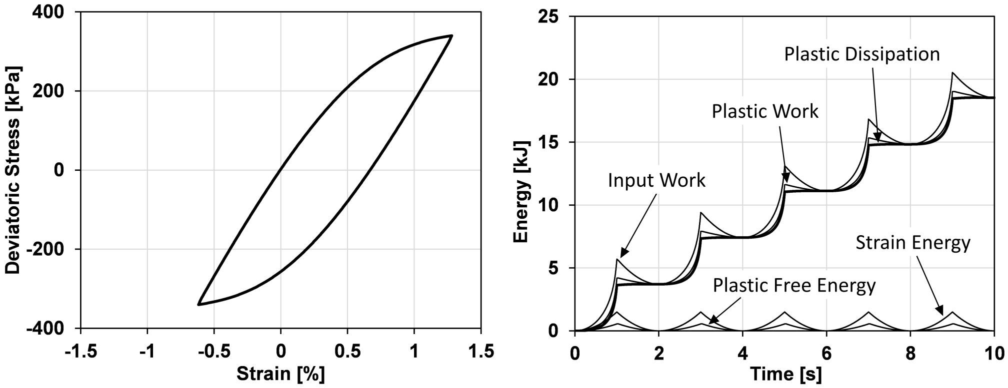

(a) (b)

Figure 9: Energy analysis of elastic-plastic material with Armstrong-Frederick kinematic hardening: (a) Stress-strain diagram; (b) Input work, plastic dissipation, strain energy, and plastic work.

List of Tables

Table 1: Energy analysis results for linear elastic materials (single element).

Case	Material Property		Simulation Results						
	E (GPa)	ν	u (m)	$\boldsymbol{W_{Input}}$ (J)	E_K (J)	E_S (J)	E_P (J)	$\boldsymbol{E_{Stored}}$ (J)	$\boldsymbol{D_P}$ (J)
1a	100	0.30	2.60E-5	13.00	0.00	13.00	0.00	13.00	0.00
1b	150	0.30	1.73E-5	8.67	0.00	8.67	0.00	8.67	0.00
1	200	0.30	1.30E-5	6.50	0.00	6.50	0.00	6.50	0.00
1c	250	0.30	1.04E-5	5.20	0.00	5.20	0.00	5.20	0.00
1d	300	0.30	8.67E-6	4.33	0.00	4.33	0.00	4.33	0.00
1e	200	0.20	1.20E-5	6.00	0.00	6.00	0.00	6.00	0.00
1f	200	0.25	1.25E-5	6.25	0.00	6.25	0.00	6.25	0.00
1	200	0.30	1.30E-5	6.50	0.00	6.50	0.00	6.50	0.00
1g	200	0.35	1.35E-5	6.75	0.00	6.75	0.00	6.75	0.00
1h	200	0.40	1.40E-5	7.00	0.00	7.00	0.00	7.00	0.00

Table 2: Energy analysis results for linear elastic materials (cantilever model).

Case	Material Property		Simulation Results						
	E (GPa)	ν	u (m)	$\boldsymbol{W_{Input}}$ (J)	E_K (J)	E_S (J)	E_P (J)	$\boldsymbol{E_{Stored}}$ (J)	$\boldsymbol{D_P}$ (J)
2a	100	0.30	2.33E-3	116.57	0.00	116.57	0.00	116.57	0.00
2b	150	0.30	1.55E-3	77.71	0.00	77.71	0.00	77.71	0.00
2	200	0.30	1.17E-3	58.28	0.00	58.28	0.00	58.28	0.00
2c	250	0.30	9.33E-4	46.63	0.00	46.63	0.00	46.63	0.00
2d	300	0.30	7.77E-4	38.86	0.00	38.86	0.00	38.86	0.00
2e	200	0.20	1.20E-5	65.89	0.00	65.89	0.00	65.89	0.00
2f	200	0.25	1.26E-3	62.97	0.00	62.97	0.00	62.97	0.00
2	200	0.30	1.17E-3	58.28	0.00	58.28	0.00	58.28	0.00
2g	200	0.35	1.02E-3	51.17	0.00	51.17	0.00	51.17	0.00
2h	200	0.40	8.12E-4	40.60	0.00	40.60	0.00	40.60	0.00